1 **New class of high-contrast Fe(II) selective fluorescent probes based on**
2 **spirocyclized scaffolds for visualization of intracellular labile iron delivered by**
3 **transferrin.**
4

5 **Authors**
6 Masato Niwa,[a] Tasuku Hirayama,*[a] Kensuke Okuda,[a] and Hideko Nagasawa*[a]
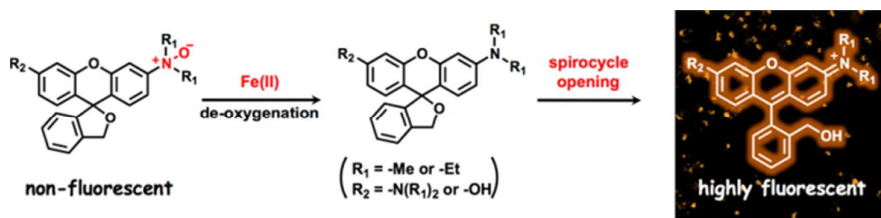7

8 **Corresponding Author**
9 Dr. T. Hirayama,
10 hirayamat@gifu-pu.ac.jp
11 Prof. H. Nagasawa
12 hnagasawa@gifu-pu.ac.jp
13 The authors declare no competing financial interest
14

20 **Abstract**
21 Iron is an essential metal nutrient that plays physiologically and pathologically important roles in biological
22 systems. However, studies on the trafficking, storage, and functions of iron itself in living samples have
23 remained challenging due to the lack of efficient methods for monitoring labile intracellular iron. Herein, we
24 report a new class of Fe^{2+}-selective fluorescent probes based on the spirocyclization of
25 hydroxymethylrhodamine and hydroxymethylrhodol scaffolds controlled by using our recently established
26 *N*-oxide chemistry as a Fe^{2+}-selective switch of fluorescence response. By suppressing the background signal,
27 the spirocyclization strategy improved the turn-on rate dramatically, and reducing the size of the substituents
28 of the *N*-oxide group enhanced the reaction rate against Fe^{2+}, compared with the first generation of the
29 *N*-oxide based Fe^{2+} probe, RhoNox-1. These new probes showed significant enhancements in the
30 fluorescence signal against not only the exogenously loaded Fe^{2+} but also the endogenous Fe^{2+} levels.
31 Furthermore, we succeeded in monitoring the accumulation of labile iron in the lysosome induced by
32 transferrin-mediated endocytosis with a turn-on fluorescence response.
33

34 **Introduction**

35   Iron is the most abundant transition metal that plays numerous essential roles in the human body.[1-3]The

36   physiological functions of iron, such as oxygen delivery, electron transport, and enzymatic reactions, rely on

37   its potent redox activity.[4-6]At the same time, iron overload can trigger severe cell damage through the

38   aberrant production of highly reactive oxygen species.[7-9] Thus, biological systems have acquired an elaborate

39   regulating machinery to maintain a well-balanced cellular iron flux. The disruption of the iron regulating

40   system potentially leads to a number of diseases, such as cancer,[10-14] hepatitis,[15] and neurodegenerative

41   diseases such as Parkinson's disease and ALS.[16, 17]Although a large portion of iron exists in the

42   protein-bound form, labile iron, which we designate to mean exchangeable, non-protein bound iron, has been

43   reported to contribute to both the healthy and diseased states in living systems.[18-20]Therefore, the need for an

44   effective method to study the biological iron has become increasingly important. In contrast withZn^{2+} and

45   Cu^+,[21-26]the development of fluorescent probes for iron remains a challenge because of its potent fluorescence

46   quenching ability as well as its multiple oxidation and spin states. Indeed, fluorescence imaging studies on

47   cellular iron have conventionally been performed with turn-off response probes, such as the commercially

48   available calcein and PhenGreen-SK, which require a significant effort to eliminate the effects of degradation

49   and clearance of the probes.[27-34]Labile iron exists as ferrous ion (Fe^{2+})rather than ferricion (Fe^{3+}) owing to its

50   greater water solubility, intracellular reductive environment, and preferable binding affinity of the

51   chaperones to Fe^{2+}.[19, 20, 35-39] Moreover, $Fe^{2+}$is a potential catalyst for the Fenton reaction, generating highly

52   harmful reactive oxygen species.[7, 40, 41] In this regard, fluorescent probes for Fe^{2+}, preferably with a turn-on

53   response, are essential for understanding both the physiological and pathological roles of the labile iron in

54   living systems. Although there are several reports of turn-on Fe^{3+} probes applicable to live cell imaging,[42-48]

55   Fe^{2+}-responsive turn-on fluorescent probes remain very rare.[34, 49-51] We have recently developed the first

56   example of a highly selective turn-on fluorescent probe for Fe^{2+}, RhoNox-1, based on a unique *N*-oxide

57   chemistry and have successfully applied it to the live cell imaging to detect endogenous labile iron.[52] Chang

58   et al. have recently developed a novel fluorogenic Fe^{2+}probe on the basis of a chelator-assisted C–O bond

59   cleavage and succeeded in monitoring iron fluctuation in the biologically stimulated models.[53]However, this

60   probe shows a similar or higher response to Co^{2+} than Fe^{2+}, and therefore, to date, our *N*-oxide strategy is still

61   the only selective and biocompatible molecular switch against Fe^{2+}. The drawback of RhoNox-1 is its basal

62   fluorescence signal ($\Phi = 0.01$), sometimes causing a background signal in imaging applications. The *N*-oxide

63   of RhoNox-1 acts as a fluorescence quencher through photo-induced electron transfer (PET) and twisted

64   internal charge transfer (TICT) and as a trigger of Fe^{2+}-mediated reaction. Furthermore, we found that the

65   *N*-oxidation of diethylamino group of rhodamine B could stabilize the spirolactone structure by shifting an

66   open–closed equilibrium, wherein RhoNox-1 is present as non-fluorescent closed spirolactone in the basic

67   region (pH > 11.5), while rhodamine B exists as a fluorescent opened quinoid structure in aqueous media

68   independent of pH. Kamiya et al. established a controlled spirocyclization of a rhodol scaffold using a

69   phenolic *O*-alkylation to achieve highly sensitive fluorescence detection of *β*-galactosidase activity with an

70   enhanced off/on contrast.[54]To overcome the background signal of RhoNox-1 and obtain a high contrast

71   fluorescence response, we anticipate that the *N*-oxidation of a dialkylamino group in

72   hydroxymethylrhodamines and hydroxymethylrhodols can control the open–closed equilibrium to the

73   non-fluorescent spirocyclic structure at physiological pH, while the corresponding deoxygenated dyes exist

74   in the predominantly fluorescent open form (Scheme 1a), which would provide a better off/on contrast than

75   RhoNox-1.In this context, we designed a new class of Fe^{2+} fluorescent probes (Scheme 1b) by utilizing the

76   *N*-oxide as a dual function molecular switch capable of sensing Fe^{2+} and modulating spirocyclization. This

77   spirocyclization/*N*-oxide strategy improved the probe's performance regarding to response rate as well as

78   turn-on rate and enabled visualization of transferrin-delivered intracellular labile iron by using the most

79   effective probe.
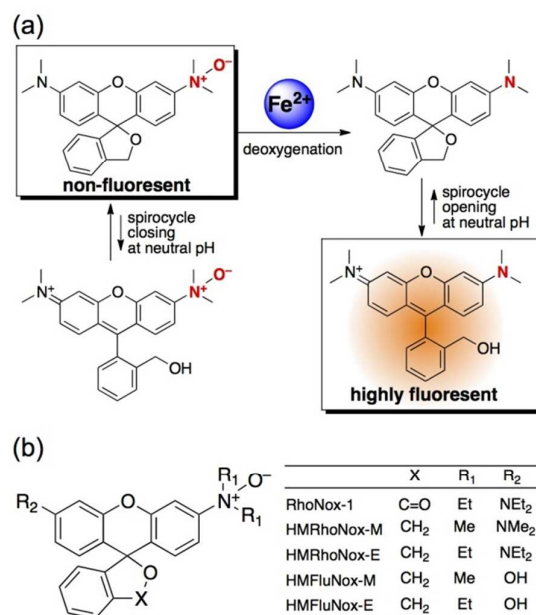
80

81   ***Scheme 1***. (a) Detection mechanism for Fe^{2+} based on *N*-oxide-controlled spirocyclization.

82   HMRhoNox-M is shown as a representative. (b) Structures of RhoNox-1, HMRhoNox-M,

83   HMRhoNox-E, HMFluNox-M, and HMFluNox-E.

84

85   **Synthesis**

86   To establish an *N*-oxide-based strategy to regulate spirocyclization, we designed four *N*-oxide compounds as

87   Fe^{2+} probes: HMRhoNox-M, HMRhoNox-E, HMFluNox-M, and HMFluNox-E (Scheme 1) containing the

88   chromophores   of   tetramethylhydroxymethylrhodamine   (HMRhodamine-M),

89   tetraethylhydroxymethylrhodamine (HMRhodamine-E), dimethylhydroxymethylrhodol (HMRhodol-M), and

90   diethylhydroxymethylrhodol (HMRhodol-E), respectively. The presence of a dimethylamino group instead

91   of the diethylamino group was explored to determine whether steric hindrance could affect the response rates

92   against Fe^{2+}. All the chromophore components were synthesized according to the previously reported

93   procedures.[54-57]The *N*-oxidation of the dyes with *m*-chloroperbenzoic acid provided the corresponding

94   *N*-oxide compounds, HMRhoNox-M, HMRhoNox-E, HMFluNox-M, and HMFluNox-E. All the *N*-oxide

95   compounds were obtained as colorless or pale-colored solids, suggesting that these probes exhibit a

96   spirocylclic structure rather than an open quinoid form, which would exhibit a strong color due to the

97   conjugated xanthene structure. The presence of a spirocyclic structure is also supported by the[1]H-NMR

98   spectra (see supporting information). The peaks assigned to the *ortho*-position of the dialkylamino group for

99   the HMRhoNox series and those of hydroxyl group for HMFluNox series appeared at approximately6.5 ppm.

100   The relatively low chemical shift values of the aromatic protons are comparable to those of the spirolactone

101   form of RhoNox-1(6.5 ppm).[52]

102

103   **Evaluation of open–closed structure by UV-vis spectra measurements**

104   We first evaluated the spirocyclization equilibrium of the new probes as well as the corresponding dyes by

105   UV-vis spectra measurements at various pH (Figure S1).The pH profiles of each visible absorption band

106   provide a pK_{cycl}, defined as the pH where the absorbance decreases to half the maximum value due to

107   spirocyclization (Figure 1). HMRhoNox-M and HMRhoNox-E exhibited a $pK_{cycl}$of 4.7 and 5.6, respectively,

108   indicating that they exist in the open quinoid form only under acidic conditions(pH < 5) and in the closed

109   spirocyclic form above pH 6 (Figure 1a, b). The pK_{cycl} of HMFluNox-M and HMFluNox-E could not be

110   determined because of their negligible visible absorbance for the entire tested pH range (Figure S1e, g). This

111   result indicates that both HMFluNox-M and HMFluNox-E are generally in the spirocyclic form in an

112   aqueous solution. In contrast, the corresponding dyes, HMRhodamine-M, HMRhodamine-E, HMRhodol-M,

113   and HMRhodol-E, exhibit pK_{cycl} of 9.3, 8.5, 11.0, and 11.3, respectively, as well as an intense absorbance

114   derived from the open quinoid form below pH 8 (Figure 1, black circles, and Figure S1b, d, f, h).[54]These data

115   suggest that the new N-oxide probes exist in a non-fluorescent spirocyclic state under the physiological pH

116   range, while the corresponding dyes are highly fluorescent due to the open quinoid configurations.

117   Consequently, a structurally controlled fluorogenic response to Fe^{2+} is likely to occur as a result of the

118   dramatic shift in the spirocyclization equilibrium caused by the N-oxidation.

119

120
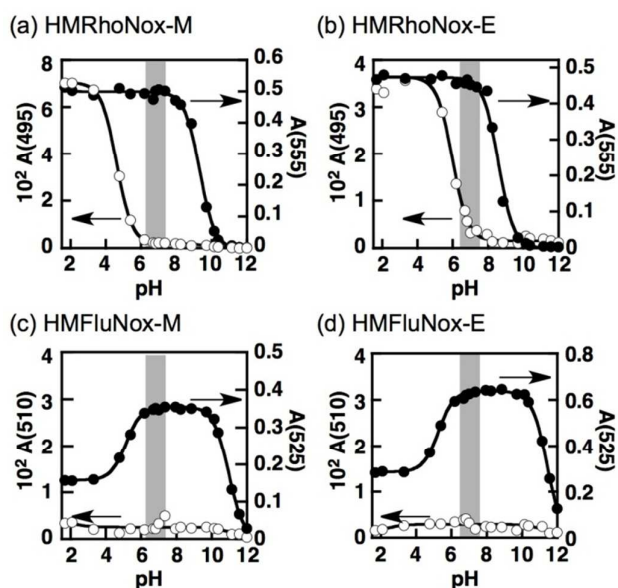
121

122   *Figure 1*. Plots of absorbance at each maximal wavelength in visible region against pH. (a)

123   HMRhodamine-M (black) and HMRhoNox-M (white), (b) HMRhodamine-E (black) and

124   HMRhoNox-E (white), (c) HMRhodol-M (Black) and HMFluNox-M (white), and (d)

125   HMRhodol-E (black) and HMFluNox-E (white). These data were acquired with 5μM probe or dye

126   at 25 °C. Physiological pH range is highlighted with gray.

127

128

129

130   **Fluorescence responses and metal selectivity tests**

131   We examined the fluorescence response of the *N*-oxide probes upon Fe^{2+} in HEPES buffer (pH 7.4).

132   HMRhoNox-M and HMRhoNox-E showed only negligible fluorescencein an aqueous buffer before the

133   introduction of Fe^{2+}(Figure 2a, b).The addition of Fe^{2+}induced a 60-fold increase in the fluorescence signal at

134   575 nmfor both probes after incubation of 1 h. Compared with RhoNox-1 (a 30-fold increase after 1 h), the

135   turn-on contrasts were significantly improved due to the extremely low basal signals derived from the closed

136   spirocyclic structures under physiological conditions. The response rate of HMRhoNox-M is higher than

137   those of HMRhoNox-E and RhoNox-1 due to the lower steric hindrance of the methyl substituent compared

138   with the ethyl group. The rhodol-based probes, HMFluNox-M and HMFluNox-E also exhibited a 40-fold

139   and a 4.5-fold change in the turn-on response at 535 nm against Fe^{2+}, respectively (Figure 2c, d).In the case

140   of the hydroxymethylrhodamine-based probes, the response rate of the N-methyl derivative, HMFluNox-M,

141   was also improved compared with that of RhoNox-1 and HMFluNox-E with the ethyl substituent. On the

142   basis of the change in the absorbance spectra with the extinction coefficients of the corresponding dyes

143   (Figure S1), the reactions' yields were estimated to be approximately 26%, 21%, 14%, and 2.5% for

144   HMRhoNox-M, HMRhoNox-E, HMFluNox-M, and HMFluNox-E, respectively, after 1 h incubation in the

145   presence of Fe^{2+}(Figure S2). LC-MS analysis of the reaction mixtures revealed that in addition to the

146   corresponding deoxygenated dyes, a trace amount of byproducts, which were assumed to be

147   mono-dealkylated dyes, were also observed in the reaction mixture (Figure S3).The dealkylated products

148   might be the result of a Meizenheimer-type rearrangement[58] followed by Fe^{2+}-induced N–O bond cleavage; a

149   detailed mechanistic study of this transformation remains on going.

150

151

152
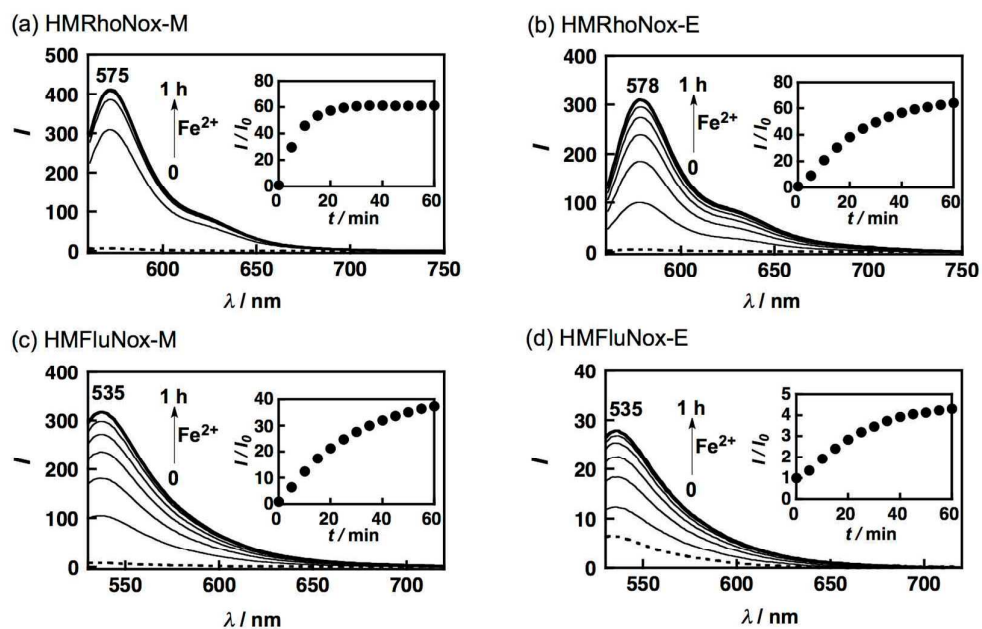
Figure 2. Fluorescence spectra of (a) HMRhoNox-M, (b) HMRhoNox-E, (c) HMFluNox-M, and (d) HMFluNox-E at 0, 10, 20, 30, 40, and 60 min after addition of 20 μM Fe^{2+}. Dotted lines and bold lines indicate fluorescence spectra at 0 min and 60 min, respectively. The insets represent the plots of relative fluorescence intensity at 575 nm (a, b) and 535 nm (c, d) against time. All the data were acquired with 2 μM probe in 50 mM HEPES buffer (pH 7.4, 0.2% DMF) at 25 °C under an Ar atmosphere. $Fe(NH_4)_2(SO_4)_2 \cdot 6H_2O$ was used as a ferrous ion source. Excitation was provided at 550 nm (a, b) or 515 nm (c, d).

The fluorescence responses of HMRhoNox-M, HMRhoNox-E, HMFluNox-M, and HMFluNox-E are highly selective for Fe^{2+} over other transition metal ions, including Fe^{3+}, alkali metal ions, and alkaline earth metal ions (Figure 3).The addition of biologically relevant reductants and reactive oxygen species to the probes also resulted in only a negligible response(Figure S4). In particular, inactivity against glutathione and cysteine, which are very abundant biological reductants, is essential for decreasing the background signal in live-cell imaging applications. Altogether, these results suggest that the new *N*-oxide fluorescence switching system for the selective Fe^{2+} detection potentially works not only for rhodamine-based dyes but also for a wide variety of chromophores bearing a tertiary aryl amine moiety.

169
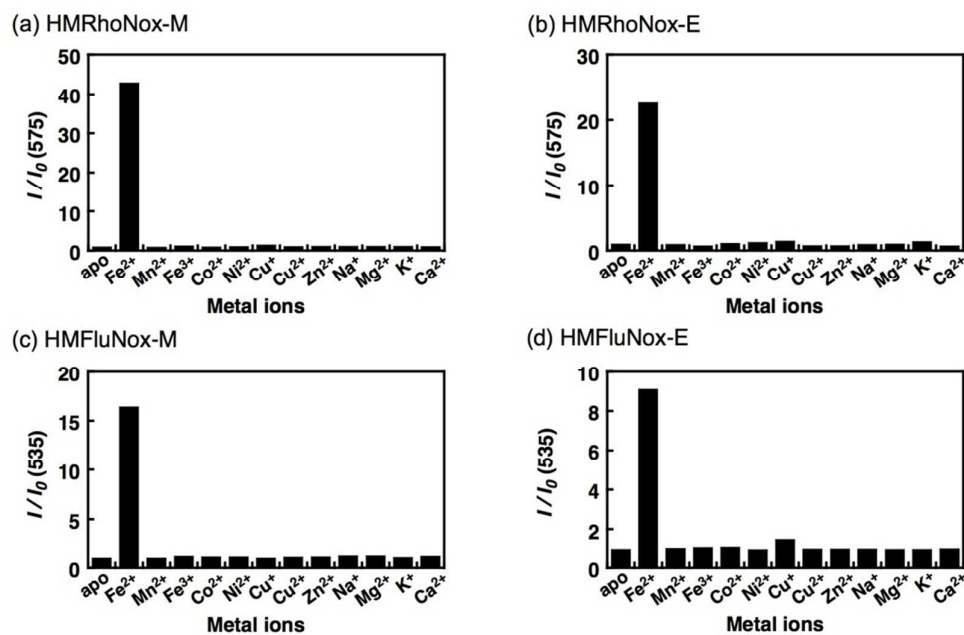
Figure 3. Fluorescence response of 2 μM (a) HMRhoNox-M (b) HMRhoNox-E (c) HMFluNox-M
(d) HMFluNox-E upon addition of various metal ions (1 mM for Na$^+$, Mg^{2+}, K$^+$, and Ca^{2+}, and 20
μM for all other metal ions). All the data were acquired in 50 mM HEPES buffer (pH 7.4, 0.2%
DMF). Bars represent relative fluorescence intensities at 575 nm (a, b, λ_{ex} = 550 nm) and 535 nm (c,
d, λ_{ex} = 515 nm).

Imaging study

Next, we applied these probes to perform live-cell imaging of human hepatocellular carcinoma cells (HepG2
cells). Prior to the imaging study, to improve their membrane-permeability, HMFluNox-M and
HMFluNox-E were converted into the acetylated forms, Ac-HMFluNox-M and Ac-HMFluNox-E,
respectively. The acetyl group is readily cleaved by intracellular esterase. Representative images are shown
in Figure 4.Compared with the control cells incubated without Fe^{2+},a significant increase in the fluorescence
signal was observed as a punctate staining pattern in the Fe^{2+}-treated cells when HMRhoNox-M and
HMRhoNox-E were used (Figure 4 a2 and b2).Ac-HMFluNox-M and Ac-HMFluNox-E also exhibited signal
enhancements as a result of the Fe^{2+} treatment (Figure 4 c2 and d2). To confirm if the observed signal
enhancements reflect the intracellular Fe^{2+} level, we performed a chelating experiment by using
2,2'-bipyridyl (Bpy) as a membrane-permeable Fe^{2+}-selective chelator.[59, 60]Prior to the live cell study, we
confirmed that Bpy could completely suppress the fluorescence response against Fe^{2+}*in vitro* for all the
probes (Figure S4a-d, entry 12). As seen in the *in vitro* test, the treatment of the Fe^{2+}-supplemented cells with
Bpy resulted in an attenuation of the signal to the basal level for all the probes (Figure 4a3, b3, c3, and d3).
Furthermore, Bpy-treated cells that were not supplemented with Fe^{2+}exhibiteda significantly lower
fluorescence signals than the control cells when HMRhoNox-M, HMRhoNox-E, or Ac-HMFluNox-M was
used (Figure 4 a4, b4, and c4). These results indicate that the probes, with the exception of Ac-HMFluNox-E,
are potentially able to monitor the endogenous Fe^{2+}fluctuations in living cells. All the new probes respond to
Fe^{2+} in a dose-dependent manner (Figure S5).Although HMRhoNox-M and HMRhoNox-E are quite

194   sensitive in the cuvette as shown in Figure 2, their detection limits in live cell applications are not

195   dramatically improved compared with RhoNox-1 (ca. 10 μM), which might be due to a different subcellular

196   distribution (*vide infra*).Meanwhile, the sensitivities of Ac-HMFluNox-M and Ac-HMFluNox-E in live cell

197   application were comparable to that of RhoNox-1. The nuclear staining and bright field images show that the

198   cells looked healthy during these imaging experiments, which indicates the low toxicity of these probes

199   (Figure 4, a5–a8, b5–b8, c5–c8, and d5–d8). Next, a series of co-staining experiments revealed the

200   subcellular localization of each probes. HMRhoNox-M and HMRhoNox-E were mainly localized in

201   lysosome (Figure S6a, b) as expected from the punctate staining patterns. On the other hand,

202   Ac-HMFluNox-M and Ac-HMFluNox-E showed endoplasmic reticulum distribution (Figure S6c, d).

203   Because the lysosome is known as an acidic organelle,[61, 62] we were concerned that the possibility of the

204   emission signals detected in HMRhoNox-M and HMRhoNox-E might be caused by the spirocycle opening

205   due to pH alteration. The pH titrations of emission intensities of HMRhoNox-M and HMRhoNox-E revealed

206   that only negligible fluorescence signal enhancement occur at the acidic region (Figure S7b, d). Furthermore,

207   Fe^{2+}-triggered fluorescence enhancement was not affected by the acidic conditions (pH 5, Figure S7a, c).

208   From the pH profiles in Figure 1a and 1b,the ratios of the opened structure for the HMRhoNox-M and

209   HMRhoNox-E probes were estimated to be approximately30% and 80%, respectively. The significantly

210   lower than expected emission from that of the opened structure might be due to intrinsic fluorescence

211   quenching property of the *N*-oxide through PET and/or TICT as observed in RhoNox-1. Consequently, the

212   fluorescence signal's enhancement in the Fe^{2+}-supplemented cells is definitely not attributed to the

213   pH-dependent spirocycle opening of the probes but to the generation of HMRhodamine dyes through the

214   selective Fe^{2+}-mediated deoxygenation.

215
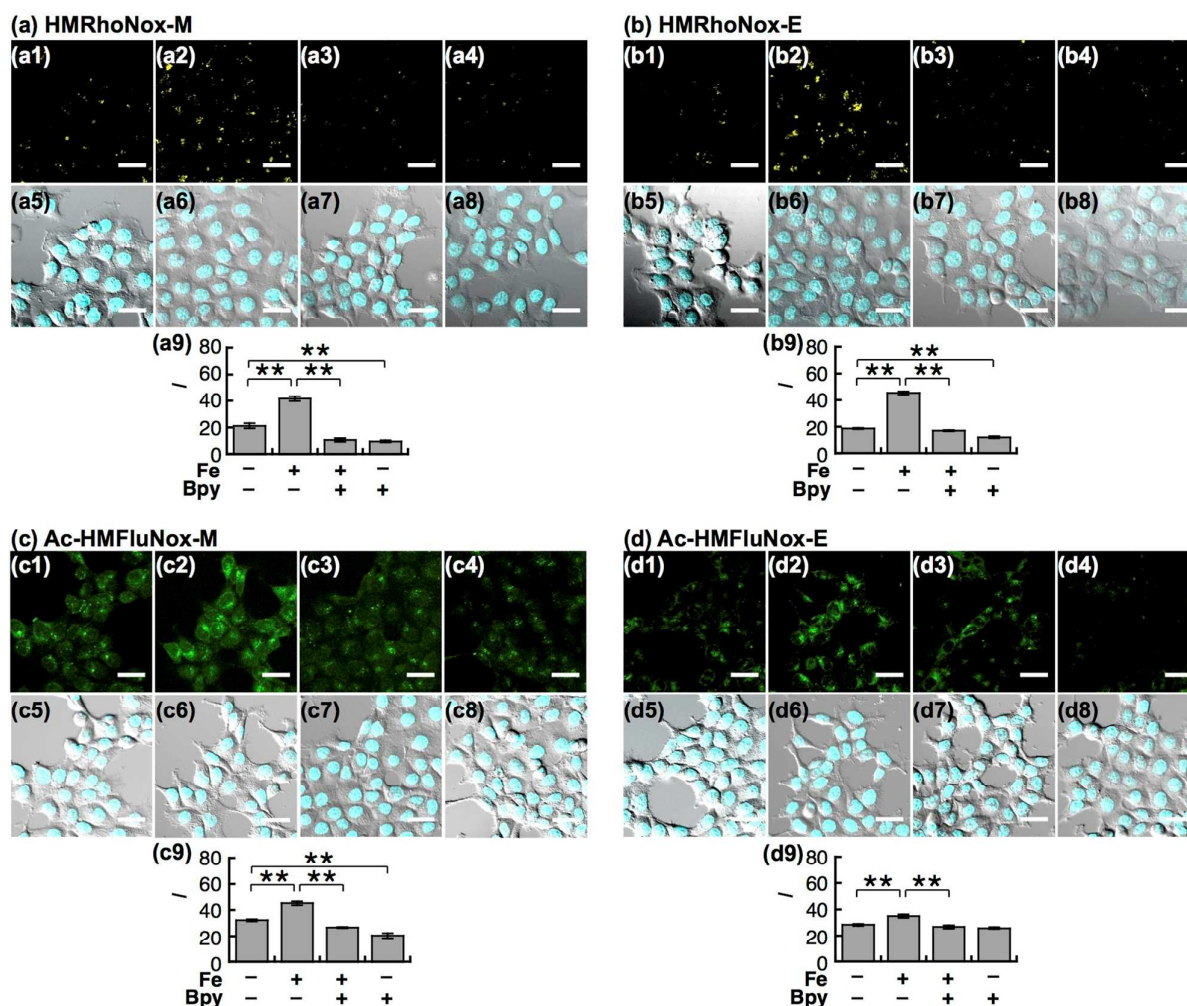
Figure 4. Confocal fluorescence microscopy images for Fe^{2+} detection in HepG2 cells by using (a) HMRhoNox-M, (b) HMRhoNox-E, (c) Ac-HMFluNox-M, or (d) Ac-HMFluNox-E. (1) Images of HepG2 cells treated with probe at 37 °C for 1 h. (2) Images of the cells supplemented with 100 μM Fe^{2+} at37 °C for 30 min and then treated with probe at 37 °C for 30 min. (3) Images of the cells treated with 100 μM Fe^{2+} at 37 °C for 30 min, and then 1 mM 2,2'-bipyridyl (Bpy) and probe at 37 °C for 30 min. (4) Images of the cells treated with 1 mM Bpy and probe at 37 °C for 30 min. (5), (6), (7), (8) Bright field images overlaid with nuclear staining (Hoechst 33342) for the same slices of (1), (2), (3), and (4), respectively. (9) Quantification of data in (1), (2), (3), and (4). Statistical analyses were performed with a Student's *t*-test. **$P < 0.01$, (n = 3). Error bars show ± s.e.m. Scale bars indicate 30 μm. All the data were acquired with the probe concentration of 1 μM (for HMRhoNox-M and HMRhoNox-E) and 5 μM (for HMFluNox-M and HMFluNox-E) and by using ferrous ammonium sulfate, Fe(NH$_4$)$_2$(SO$_4$)$_2$•6H$_2$O (FAS) for Fe^{2+} source. Excitation was provided with 555 nm laser for (a)and (b) or 488 nm laser for (c) and (d).

Monitoring transferrin-induced Fe uptake

After establishing that the HMRhoNox series are able to reliably detect intracellular Fe^{2+} levels, we used HMRhoNox-M to monitoring iron ingress triggered by the iron-chelating protein, transferrin (Tf). The

9

233   Tf-mediated iron uptake represents the primary route of cellular iron acquisition. This probe was chosen

234   because it exhibited an outstanding reaction rate and off/on signal contrast. Tf–iron complex (holoTf) is

235   internalized by the cells via receptor-mediated endocytosis of the Tf receptor (TfR).[63-65]During this process,

236   the TfR–Tf complex is delivered to the early endosome, where acidification causes the release of iron from

237   Tf as Fe^{3+}. Subsequently, Fe^{3+} is reduced to Fe^{2+} in the late endosome or lysosome and is exported into the

238   cytosol.[38, 66-68]In this context, we exploited the Fe^{2+}-selective turn-on probe to monitor the release and

239   accumulation of Fe^{2+}, which is delivered by Tf-TfR endocytosis. In Figure 5b, a significantly higher

240   fluorescence signal was observed in the cells incubated with holoTf than the control cells(Figure 5a). The

241   signal enhancement was canceled by the competitive addition of apotransferrin (apoTf) (Figure 5c),which is

242   known as an inhibitor for the binding of holoTf to TfR.[31, 69]In addition, a significantly low fluorescence

243   signal was observed when the cells were incubated at 4 °C(Figure 5d) or in the presence of NaN_3(Figure 5e),

244   where endocytosis is potently inhibited.[67, 70, 71] This experiment suggests that the increase in the signal is

245   definitely derived from the Tf-delivered iron via endocytosis. Altogether, to the best of our knowledge, this

246   imaging study, with HMRhoNox-M, is the first example of the successful visualization of Tf-induced iron

247   uptake by fluorescence imaging with a turn-on fluorescence response. The results of the study revealed that

248   the iron released from Tf could be delivered to the lysosome and accumulated in the accessible Fe^{2+} form.

249
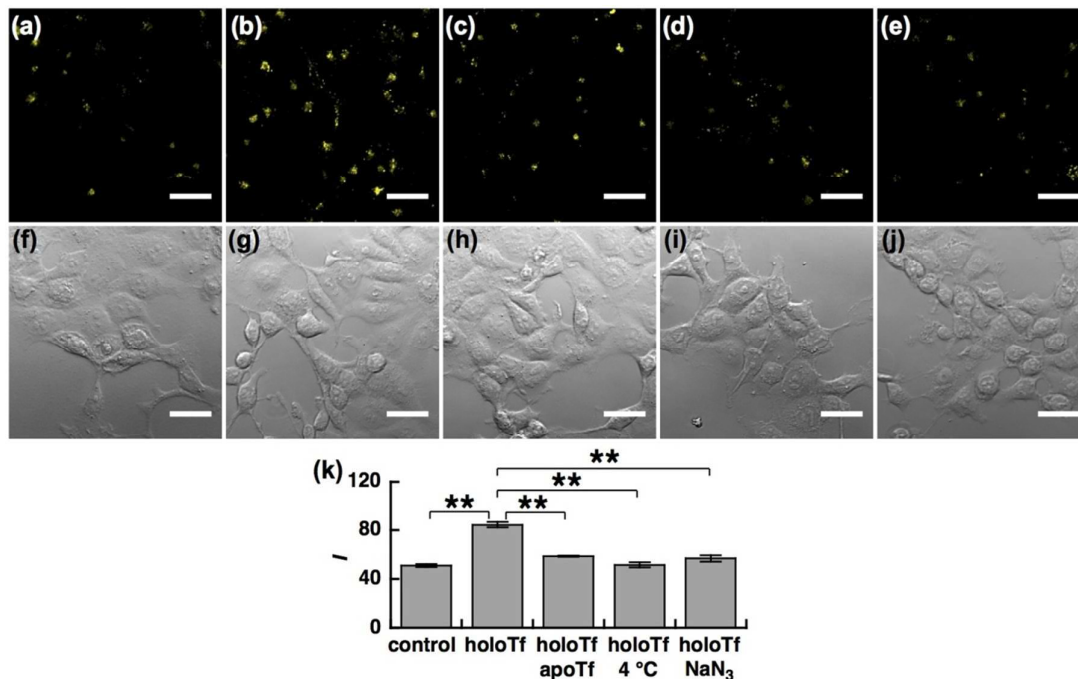
250

251   **Figure 5.** Confocal fluorescence microscopy images for monitoring Tf-induced iron uptake

252   ofHepG2 cells using HMRhoNox-M.(a) Image of HepG2 cells incubated with 1μM

253   HMRhoNox-M at 37 °C for 30 min. (b) Image of HepG2 cells supplemented with 5μM holoTf

254   at37 °C for 30 min prior to treatment with 1μM HMRhoNox-M at 37 °C for 30 min. (c) Image of

255   HepG2 cells supplemented with 5μM holoTf and 25μM apoTf at37 °C for 30 min prior to treatment

256   with 1μM HMRhoNox-M at 37 °C for 30 min.(d) Image of HepG2 cells supplemented with 5μM

257   holoTf at 4 °C for 30 min and then treated with 1μM HMRhoNox-M at 37 °C for 30 min. (e) Image

258   of HepG2 cells supplemented with 5μM holoTf and 1 mMNaN$_3$at37 °C for 30 min and then treated

259   with 1μM HMRhoNox-M at 37 °C for 30 min.(f)-(j) Bright field images for the same slices of

260   (a)-(e). (k) Quantification of data in (a)–(e). Statistical analysis was performed with a Student's

261   t-test. **$P< 0.01$(n = 3). Error bars in (g) show ± s. e. m. Scale bars indicate 30 μm.

262

Conclusion

264   In conclusion, we have designed, synthesized, and evaluated four fluorescent probes for Fe^{2+}, such as the

265   HMRhoNox and HMFluNox series using our recently established Fe^{2+}-selective caging system based on the

266   *N*-oxide chemistry for applications on hydroxymethylrhodamine and hydroxymethylrhodol scaffolds for

267   controlling spirocyclization. With the exception of HMFluNox-E, a dramatic acidic shift in the

268   spirocyclization equilibrium induced by the *N*-oxidation caused the suppression of basal fluorescence under

269   physiological conditions, thereby providing a significantly improved fluorescence response with respect to

270   the reaction rate and the off/on contrast compared with the previous probe, RhoNox-1.The live-cell imaging

271   study demonstrated that all the probes are able to visualize the intracellular Fe^{2+} by a turn-on response in a

272   dose-dependent manner. As an advanced biological experiment, the use of HMRhoNox-M afforded the live

273   cell imaging of Fe^{2+} uptake mediated by Tf-induced endocytosis. Additionally, the fact that both of the

274   rhodol-based probes, HMFluNox-M and HMFluNox-E, worked well suggests that the Fe^{2+}-selective *N*-oxide

275   fluorogenic switching system can be potentially expanded to a wide range of dyes bearing an aryl tertiary

276   amine in the chromophore. Further studies focused on improving the response rate as well as controlling the

277   subcellular localization of Fe^{2+} probes based on the *N*-oxide chemistry are in progress.

278

279

285

Supporting Information

287   Electronic supporting information (ESI) available: Synthesis and characterization of the probes, UV-vis

288   absorbance spectra, NMR spectra, pH-titration, selectivity assays, LC-MS analysis, confocal images, and

289   experimental details.

References

1.   S. J. Lippard and J. M. Berg, *Principles of Bioinorganic Chemistry*, University Science Books, 1997.

2.   P. Aisen, M. Wessling-Resnick and E. A. Leibold, *Curr. Opin. Chem. Biol.*, 1999, **3**, 200-206.

3.   M. W. Hentze, M. U. Muckenthaler and N. C. Andrews, *Cell*, 2004, **117**, 285-297.

4.   M. Costas, M. P. Mehn, M. P. Jensen and L. Que, *Chem. Rev.*, 2004, **104**, 939-986.

5.   T. A. Rouault and W.-H. Tong, *Nat. Rev. Mol. Cell Biol.*, 2005, **6**, 345-351.

6.   E. C. Theil and D. J. Goss, *Chem. Rev.*, 2009, **109**, 4568-4579.

7.   B. Halliwell and J. M. C. Gutteridge, *FEBS Lett.*, 1992, **307**, 108-112.

8.   Z. Zhang, T. Wei, J. Hou, G. Li, S. Yu and W. Xin, *Eur. J. Pharmacol.*, 2003, **467**, 41-47.

9.   A. Aroun, J. L. Zhong, R. M. Tyrrell and C. Pourzand, *Photochem. Photobiol. Sci.*, 2012, **11**, 118-134.

10.   S. J. Dixon, K. M. Lemberg, M. R. Lamprecht, R. Skouta, E. M. Zaitsev, C. E. Gleason, D. N. Patel, A. J. Bauer, A. M. Cantley, W. S. Yang, B. Morrison and B. R. Stockwell, *Cell*, 2012, **149**, 1060-1072.

11.   S. V. Torti and F. M. Torti, *Nat. Rev. Cancer*, 2013, **13**, 342-355.

12.   S. Toyokuni, *Cancer Sci.*, 2009, **100**, 9-16.

13.   C. P. Anderson, M. Shen, R. S. Eisenstein and E. A. Leibold, *Biochim. Biophys. Acta*, 2012, **1823**, 1468-1483.

14.   J. Wang and K. Pantopoulos, *Biochem. J.*, 2011, **434**, 365-381.

15.   E. Angelucci, *Blood*, 2002, **100**, 17-21.

16.   E. Madsen and J. D. Gitlin, *Annu. Rev. Neurosci.*, 2007, **30**, 317-337.

17.   L. Zecca, M. B. H. Youdim, P. Riederer, J. R. Connor and R. R. Crichton, *Nat. Rev. Neurosci.*, 2004, **5**, 863-873.

18.   L. A. Ba, M. Doering, T. Burkholz and C. Jacob, *Metallomics*, 2009, **1**, 292-311.

19.   W. Breuer, M. Shvartsman and Z. I. Cabantchik, *Int. J. Biochem. Cell Biol.*, 2008, **40**, 350-354.

20.   G. J. Anderson and C. D. Vulpe, *Cell. Mol. Life Sci.*, 2009, **66**, 3241-3261.

21.   K. Kikuchi, K. Komatsu and T. Nagano, *Curr. Opin. Chem. Biol.*, 2004, **8**, 182-191.

22.   E. Tomat and S. J. Lippard, *Curr. Opin. Chem. Biol.*, 2010, **14**, 225-230.

23.   E. L. Que, D. W. Domaille and C. J. Chang, *Chem. Rev.*, 2008, **108**, 1517-1549.

24.   L. Yang, R. McRae, M. M. Henary, R. Patel, B. Lai, S. Vogt and C. J. Fahrni, *Proc. Natl. Acad. Sci. U. S. A.*, 2005, **102**, 11179-11184.

25.   L. Zeng, E. W. Miller, A. Pralle, E. Y. Isacoff and C. J. Chang, *J. Am. Chem. Soc.*, 2006, **128**, 10-11.

26.   M. Taki, S. Iyoshi, A. Ojida, I. Hamachi and Y. Yamamoto, *J. Am. Chem. Soc.*, 2010, **132**, 5938-5939.

27.   W. Breuer, S. Epsztejn and Z. I. Cabantchik, *J. Biol. Chem.*, 1995, **270**, 24209-24215.

28.   S. Fakih, M. Podinovskaia, X. Kong, H. L. Collins, U. E. Schaible and R. C. Hider, *J. Med. Chem.*, 2008, **51**, 4539-4552.

29.   O. Kakhlon and Z. I. Cabantchik, *Free Radic. Biol. Med.*, 2002, **33**, 1037-1046.

30. U. Rauen, A. Springer, D. Weisheit, F. Petrat, H.-G. Korth, H. de Groot and R. Sustmann, *ChemBioChem*, 2007, **8**, 341-352.

31. M. Shvartsman, E. Fibach and Z. I. Cabantchik, *Biochem. J.*, 2010, **429**, 185-193.

32. F. Thomas, G. Serratrice, C. Béguin, E. S. Aman, J. L. Pierre, M. Fontecave and J. P. Laulhère, *J. Biol. Chem.*, 1999, **274**, 13375-13383.

33. P. Li, L. Fang, H. Zhou, W. Zhang, X. Wang, N. Li, H. Zhong and B. Tang, *Chem. Eur. J.*, 2011, **17**, 10520-10523.

34. K. P. Carter, A. M. Young and A. E. Palmer, *Chem. Rev.*, 2014, a.s.a.p.

35. A.-L. Bulteau, H. A. O'Neill, M. C. Kennedy, M. Ikeda-Saito, G. Isaya and L. I. Szweda, *Science*, 2004, **305**, 242-245.

36. H. Shi, K. Z. Bencze, T. L. Stemmler and C. C. Philpott, *Science*, 2008, **320**, 1207-1210.

37. I. J. Schultz, C. Chen, B. H. Paw and I. Hamza, *J. Biol. Chem.*, 2010, **285**, 26753-26759.

38. D. R. Richardson, D. J. R. Lane, E. M. Becker, M. L.-H. Huang, M. Whitnall, Y. S. Rahmanto, A. D. Sheftel and P. Ponka, *Proc. Natl. Acad. Sci. U. S. A.*, 2010, **107**, 10775-10782.

39. R. C. Hider and X. Kong, *Dalton Trans.*, 2013, **42**, 3220-3229.

40. I. Yamazaki and L. H. Piette, *J. Biol. Chem.*, 1990, **265**, 13589-13594.

41. S. Enami, Y. Sakamoto and A. J. Colussi, *Proc. Natl. Acad. Sci. U. S. A.*, 2014, **111**, 623-628.

42. R. Wang, F. Yu, P. Liu and L. Chen, *Chem. Commun.*, 2012, **48**, 5310-5312.

43. Z. Yang, M. She, B. Yin, J. Cui, Y. Zhang, W. Sun, J. Li and Z. Shi, *J. Org. Chem.*, 2012, **77**, 1143-1147.

44. M. H. Lee, T. V. Giap, S. H. Kim, Y. H. Lee, C. Kang and J. S. Kim, *Chem. Commun.*, 2010, **46**, 1407-1409.

45. M. Zhang, Y. Gao, M. Li, M. Yu, F. Li, L. Li, M. Zhu, J. Zhang, T. Yi and C. Huang, *Tetrahedron Lett.*, 2007, **48**, 3709-3712.

46. D. P. Kennedy, C. M. Kormos and S. C. Burdette, *J. Am. Chem. Soc.*, 2009, **131**, 8578-8586.

47. J. L. Bricks, A. Kovalchuk, C. Trieflinger, M. Nofz, M. Büschel, A. I. Tolmachev, J. Daub and K. Rurack, *J. Am. Chem. Soc.*, 2005, **127**, 13522-13529.

48. Y. Xiang and A. Tong, *Org. Lett.*, 2006, **8**, 1549-1552.

49. L. Praveen, M. L. P. Reddy and R. L. Varma, *Tetrahedron Lett.*, 2010, **51**, 6626-6629.

50. J.-L. Chen, S.-J. Zhuo, Y.-Q. Wu, F. Fang, L. Li and C.-Q. Zhu, *Spectrochim. Acta, Part A*, 2006, **63**, 438-443.

51. G.-G. Hou, C.-H. Wang, J.-F. Sun, M.-Z. Yang, D. Lin and H.-J. Li, *Biochem. Biophys. Res. Commun.*, 2013, **439**, 459-463.

52. T. Hirayama, K. Okuda and H. Nagasawa, *Chem. Sci.*, 2013, **4**, 1250-1256.

53. H. Y. Au-Yeung, J. Chan, T. Chantarojsiri and C. J. Chang, *J. Am. Chem. Soc.*, 2013, **135**, 15165-15173.

54. M. Kamiya, D. Asanuma, E. Kuranaga, A. Takeishi, M. Sakabe, M. Miura, T. Nagano and Y. Urano, *J. Am. Chem. Soc.*, 2011, **133**, 12960-12963.

55. S. Kenmoku, Y. Urano, H. Kojima and T. Nagano, *J. Am. Chem. Soc.*, 2007, **129**, 7313-7318.

56. S. Akita, N. Umezawa, N. Kato and T. Higuchi, *Bioorg. Med. Chem.*, 2008, **16**, 7788-7794.

57. Q. A. Best, R. Xu, M. E. McCarroll, L. Wang and D. J. Dyer, *Org. Lett.*, 2010, **12**, 3219-3221.

58. A. Albini, *Synthesis*, 1993, **1993**, 263-277.

59. F. Petrat, H. de Groot and U. Rauen, *Arch. Biochem. Biophys.*, 2000, **376**, 74-81.

60. A. M. Romeo, L. Christen, E. G. Niles and D. J. Kosman, *J. Biol. Chem.*, 2001, **276**, 24301-24308.

61. J. P. Luzio, P. R. Pryor and N. A. Bright, *Nat. Rev. Mol. Cell Biol.*, 2007, **8**, 622-632.

62. K. Glunde, S. E. Guggino, M. Solaiyappan, A. P. Pathak, Y. Ichikawa and Z. M. Bhujwalla, *Neoplasia*, 2003, **5**, 533-545.

63. E. Boucrot and T. Kirchhausen, *Proc. Natl. Acad. Sci. U. S. A.*, 2007, **104**, 7939-7944.

64. D. J. Hernández-Deviez, M. T. Howes, S. H. Laval, K. Bushby, J. F. Hancock and R. G. Parton, *J. Biol. Chem.*, 2008, **283**, 6476-6488.

65. M. Lakadamyali, M. J. Rust and X. Zhuang, *Cell*, 2006, **124**, 997-1009.

66. R. S. Ohgami, D. R. Campagna, E. L. Greer, B. Antiochos, A. McDonald, J. Chen, J. J. Sharp, Y. Fujiwara, J. E. Barker and M. D. Fleming, *Nat. Genet.*, 2005, **37**, 1264-1269.

67. J. Yang, D. Goetz, J.-Y. Li, W. Wang, K. Mori, D. Setlik, T. Du, H. Erdjument-Bromage, P. Tempst, R. Strong and J. Barasch, *Mol. Cell*, 2002, **10**, 1045-1056.

68. M. Tabuchi, T. Yoshimori, K. Yamaguchi, T. Yoshida and F. Kishi, *J. Biol. Chem.*, 2000, **275**, 22220-22228.

69. R. D. Klausner, G. Ashwell, J. V. Renswoude, J. B. Harford and K. R. Bridges, *Proc. Natl. Acad. Sci. U. S. A.*, 1983, **80**, 2263-2266.

70. S. Katayama, H. Hirose, K. Takayama, I. Nakase and S. Futaki, *J. Control. Release*, 2011, **149**, 29-35.

71. B. J. Iacopetta and E. H. Morgan, *J. Biol. Chem.*, 1983, **258**, 9108-9115.